Direct evidence of exfoliation efficiency and graphene dispersibility of green solvents towards sustainable graphene production

Kai Ling Ng[‡1], Barbara M Maciejewska[‡1], Ling Qin[2], Colin Johnston[1], Jesus Barrio[3], Maria-Magdalena Titirici[3], Iakovos Tzanakis[4], Dmitry G Eskin[5], Kyriakos Porfyrakis[6], Jiawei Mi[2], Nicole Grobert*[1,7]

[1] *Department of Materials, University of Oxford, Parks Road, Oxford, OX1 3 PH, UK*
[2] *Department of Engineering, University of Hull, Cottingham Rd, Hull, HU6 7RX, UK*
[3] *Department of Chemical Engineering, Imperial College London, South Kensington Campus, London, SW7 2AZ, UK*
[4] *School of Engineering, Computing and Mathematics, Oxford Brookes Univ., College Cl, Wheatley, Oxford, OX33 1HX, UK*
[5] *Brunel Centre for Advanced Solidification Technology, Brunel University London, Kingston Lane, UB8 3PH, UK*
[6] *Faculty of Engineering and Science, University of Greenwich, Central Avenue, Chatham Maritime, Kent, ME4 4TB, UK*
[7] *Williams Advanced Engineering, Grove, Oxfordshire, OX12 0DQ, UK*

KEYWORDS graphene, liquid phase exfoliation, green solvents, NMP, exfoliation efficiency, dispersibility, re-dispersion

ABSTRACT: Achieving sustainable production of pristine high-quality graphene and other layered materials at low cost is one of the bottlenecks that needs to be overcome for reaching 2D materials applications at scale. Liquid Phase Exfoliation (LPE) in conjunction with N-methyl-2-pyrrolidone (NMP) is recognised as the most efficient method for both the exfoliation and dispersion of graphene. Unfortunately, NMP is neither sustainable nor suitable for up-scaling production due to its adverse impact on the environment. Here we show the real potential of green solvents by revealing the independent contributions of their exfoliation efficiency and graphene dispersibility to the graphene yield. By experimentally separating these two factors we show that the exfoliation efficiency of a given solvent is independent of its dispersibility. Here we show that isopropanol can be used to exfoliate graphite as efficiently as NMP. Our finding is corroborated by the matching ratio between the polar and dispersive energy of graphite and that of the solvent surface tension. This direct evidence of exfoliation efficiency and dispersibility of solvents paves the way to developing a deeper understanding of the real potential of sustainable graphene manufacturing at scale.

INTRODUCTION

Graphene is widely investigated as next generation material for application in flexible electronics,[1] electrocatalysts,[2] bioscaffolds,[3] and sensors[4] *etc*. For such applications, graphene is generally produced by simple, scalable, and inexpensive liquid phase exfoliation (LPE) techniques whereby graphite crystals are either shear mixed (SM) or ultrasonically exfoliated (US) in a solvent. In LPE, there are three key factors that influence and govern the graphene yield: the i) graphite quality, and the ii) exfoliation efficiency, and iii) dispersibility of the solvent. The quality of graphite, defined by graphite size, crystallinity, and impurities, greatly affects its wettability[5–7] The higher the graphite quality, the lower its wettability is, and if a solvent cannot wet the graphite, it cannot enter between the graphite layers to peel them off. Intuitively, this means that large, highly crystalline graphite flakes are more difficult to exfoliate than smaller, less crystalline and defect-containing graphite powders. The exfoliation efficiency is defined by the ability of the solvent to 'peel off' individual layers of graphene from the graphite crystal. In contrast to this, the graphene dispersibility is the ability of the solvent to form uniform and stable graphene dispersions over a given time. Typically, 1-methyl-2-pyrrolidone (NMP) or dimethylformamide (DMF) is used as solvent in LPE since both are ideal for exfoliating graphite and producing stable dispersions of graphene[8]. However, their toxicity and high boiling points, *e.g.*, 153 ˚C and 202 ˚C for DMF and NMP respectively, are an issue in the context of sustainable graphene manufacturing, and therefore, alternative LPE solutions must be sought out.[9–14] High-boiling point solvents are difficult to remove and result in major loss of material, degradation of material quality and the generation of toxic waste.[13,15,16] Therefore, major significant efforts have gone into finding suitable and sustainable solvent alternatives, so-called green solvents.[13, 17] Green solvents are eco-friendly solvents with low boiling points, *e.g.*, < 100 ˚C, and low toxicity.[18] Although previous work has shown that green solvents can indeed be used to produce graphene by means of LPE, it has not progressed much further. To enhance the graphene yield in green solvent LPE (GS-LPE), which currently is *ca.* 50-75% lower than in DMF or NMP,[19, 20]additives such as surfactants and/or dispersants (sodium cholate, sodium dodecylsulfate, pluronic, *etc.*) have been intensively explored.[21–24] Unfortunately, additives remain on the graphene and are difficult to remove after exfoliation, and therefore the as-produced graphene is no longer pristine, which can affect its properties and negatively influence its performance.[25] In the pursuit of improving the graphene yield of the GS-LPE process, solvent exchange methods have also been investigated, whereby graphite was first 'pre-treated' and/or exfoliated in NMP or DMF, followed by redispersion of the as-produced graphene in a green solvent. [26–28] While the graphene yield could indeed be increased through the solvent exchange, toxic NMP and DMF solvents are still required for the exfoliation. To overcome the current limitations of GS-LPE, it is important to develop an understanding of the actual role that the solvent plays in the LPE mechanism, and how it specifically contributes towards the exfoliation process. To establish the mechanism of graphite GS-LPE, the exfoliation efficiency and the dispersibility of green solvents must be studied independently, because the evaluation of the true graphene yield in green solvents is hindered by the limited dispersibility of as-produced graphene in green solvents. The low amount of collected (and detected) graphene gives the false impression that green solvents are unsuitable for the efficient production of graphene. This study paves the way for the development of a set of post-exfoliation procedures for the enhancement of the graphene yield in green solvents through the optimisation of their dispersibility. This route opens up new opportunities to explore the real potential of green solvents, thought of as inefficient in the production of graphene via LPE.

RESULTS AND DISCUSSION

To study the feasibility of replacing NMP and DMF with green solvents (S1.1), we employed shear mixing LPE (SM-LPE, S1.2) in conjunction with distinctively different graphite materials, *i.e.*, graphite platelets (G150) and graphite powder (G50) with lateral

sizes of 150 µm and 50 µm respectively, and their surface areas of 13.15 m^2/g (G150) and 1.88 m^2/g (G50) were measured by Brunauer-Emmet-Teller (BET) N_2 absorption isotherms (Fig.1a). The experimental methods used for exfoliation and redispersion of the exfoliated graphene are detailed in S1.2. The characterisation technique used for the graphite and graphene materials are detailed in S2. Following the work by Coleman *et al.*, it is generally accepted that higher graphene yield can be achieved if the surface tension or solubility parameters of a solvent is similar to that of graphene.[11, 29] This rule-of-thumb is typically employed to select the solvents for LPE of layered materials.[30] The surface energy of ideal graphene, *i.e.* atomically perfect graphene, is 68 mJ/m^2.[31, 30] This value changes for defective graphene, and may vary for graphite due to, for example, graphite morphology, lateral size, defect density, edge defects, d-spacing, additional functional groups, *etc.*.[32, 5] We deliberately selected graphite starting materials with different degree of defect in our study. G50 graphite is more defective than G150, with higher D peak at (1350 cm^{-1} raman shift), as analysed through the Raman spectroscopy (S3). Herein, we employed SM-LPE in a range of green solvents (Ace, MeOH, EtOH, IPA, EA, IPA, and (1:1) mixtures of EtOH:D.I. and IPA:Ace) while keeping shear mixing parameters constant (S1.2.1). As the shear mixing product usually consists of well-separated/dispersed graphene and graphite aggregates composed of stacked graphene and partially exfoliated graphite (Fig. 1b), the centrifugation is employed to separate the graphene-rich phase from other exfoliation products. If the solvent dispersibility is poor, however, as in the case for graphene in green solvents, the exfoliated graphene starts to restack and sediments during centrifugation. In such a case, the graphene collected in the supernatant phase is much lower than the actual amount of graphene originally exfoliated, and the graphene concentration is limited to the amount that a given green solvent can disperse. For example, if the same amount of graphene is dispersed in two solvents (A and B) with different graphene dispersibility, where solvent B has higher dispersibility, the concentration of graphene measured from the supernatant solvent B, would be higher than that of solvent A, (Fig. 1c) and therefore would distort the measurement of the actual graphene concentration.

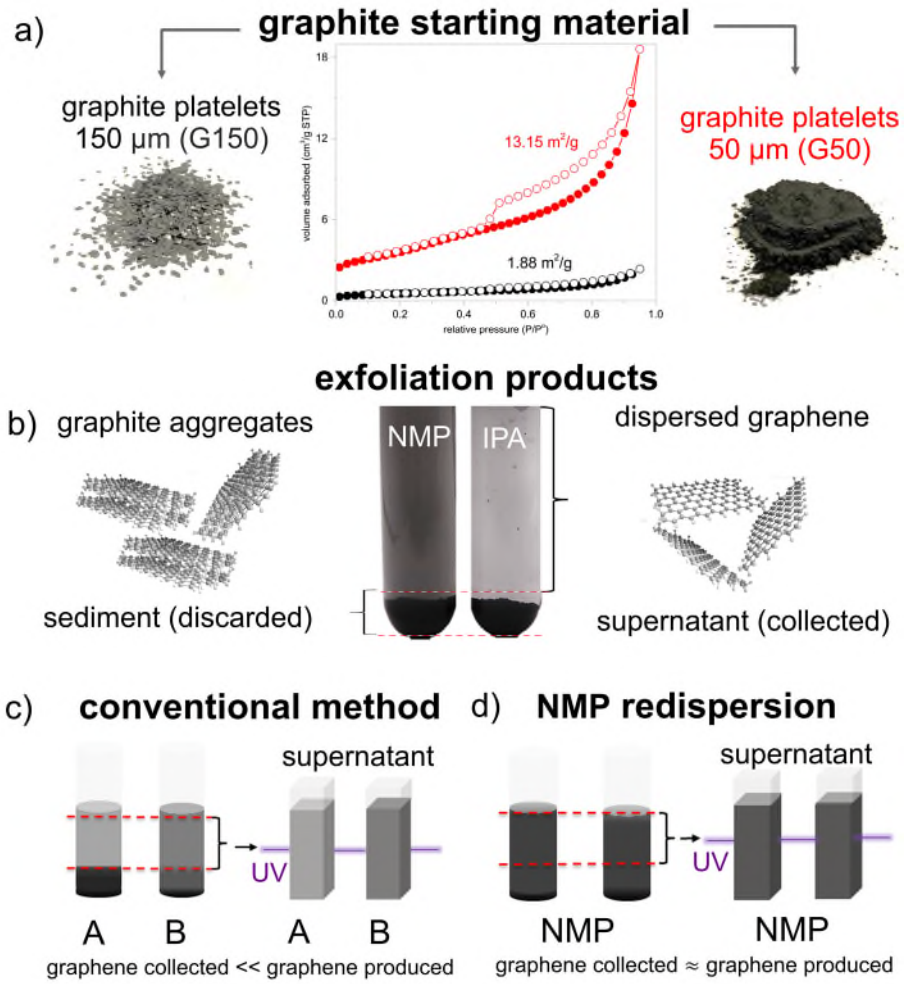

Fig. 1: *a) Digital images of graphite platelets (150 µm; G150) and powder (50 µm; G50); Brunauer-Emmet-Teller surface area evaluation of both; b) Centrifuge tubes with a fixed amount of exfoliation product containing graphite aggregates and graphene dispersed in NMP and IPA respectively. When the exfoliation product contains the same amount of graphene, solvents with a higher graphene dispersibility result in higher concentrations of graphene collected from the supernatant. c) For the conventional method, the concentration characterised is limited by the graphene dispersibility in the solvent. Due to the lower graphene dispersibility in solvent A, the exfoliated graphene restacks and sediments during centrifugation. This results in a lower amount of graphene being collected from the supernatant, and thus, a lower concentration is measured, despite the same initial amount of graphene content as in solvent B. d) The NMP redispersion (NMP-R) method makes use of the higher graphene dispersibility of NMP to minimise graphene restacking, so that the graphene produced remains well-separated in the supernatant.*

To study the green solvent exfoliation efficiency and dispersibility of graphene independently, we performed SM-LPE in a range of green solvents, then removed the solvent and re-dispersed the subsequent powder in NMP (with high dispersibility) for analysis only, referred to as the NMP-re-dispersion (NMP-R) from hereon. Here, NMP merely serves as a standardised dispersing medium to investigate both, the exfoliation efficiency and dispersibility, independently. With this approach it was possible to compare the

actual exfoliation efficiency of the green solvents studied. For the study of the green solvent dispersibility however, an inverse approach was taken, namely the green solvent re-dispersion (GS-R). For the GS-R, graphite was first exfoliated in NMP, next the LPE product was washed and dried, and then re-dispersed in green solvents. In both cases, a vortex mixer was used for the re-dispersion, *i.e.*, no ultrasound or shear mixing was applied. (Fig. 1d). The detailed experimental procedures of NMP-R and GS-R are presented in S1.2. Both, NMP-R and GS-R routes can be applied to any type of graphite or other layered materials in order to identify the most efficient green solvent for the synthesis of these materials. UV-vis absorption spectra are the most frequently used for the evaluation of the actual graphene concentration and consequently graphene yield. In order to estimate the graphene concentration, the absorptivity value of graphene in a given solvent is required. It is a common practice to use the absorptivity values generated from calibration using only a single solvent medium, which is then used for concentration calculation in various solvent media. In the literature, the type of solvent medium used for making a calibration curve for absorptivity value is often not specified. [17,30,33,34] Here, we show the significance of selecting the right dispersing solvent medium for the calibration curve to generate a reliable standardised absorptivity value for concentration calculation that can be applied to different dispersing solvent media used. We compared the absorptivity values for GR150 and GR50 in both NMP and D.I. (see Fig. S4a, b). Moreover, in most cases, the graphene yield or exfoliation efficiency is correlated with the initial weight of graphite used for LPE, and it is generally accepted that the graphite source is represented by its mass,[35] whilst the graphite surface area is neglected or not considered to be important. For example, Lund *et al*., claimed that the concentration of graphene produced using LPE is independent on the size of the graphite source.[36] Here we demonstrate that the nature of the starting graphite material matters, because the exfoliation efficiency and dispersibility are greatly affected by the crystallinity (*e.g.*, d-spacing) and size of the graphite crystal. Both, the conventional GS-LPE (Fig. 2a) and the GS-LPE combined with the NMP-R approach (Fig. 2b), showed that the estimated mass per surface area for GR50 is much lower than that of GR150. This is most likely due to the much larger lateral size of G150 exposed to the direction parallel to shear force generated between rotor and stator during LPE. This indicates the importance of considering the quality of the graphite starting materials in the evaluation of LPE process capability to exfoliate graphene. Here, we normalised the graphene concentration and divided the mass of exfoliated graphene by the surface area of the initial graphite source (Fig. 2) in order to emphasize the structural difference between types of graphite used (see also S5 that showed the conventional method of concentration analysis without surface area normalisation).

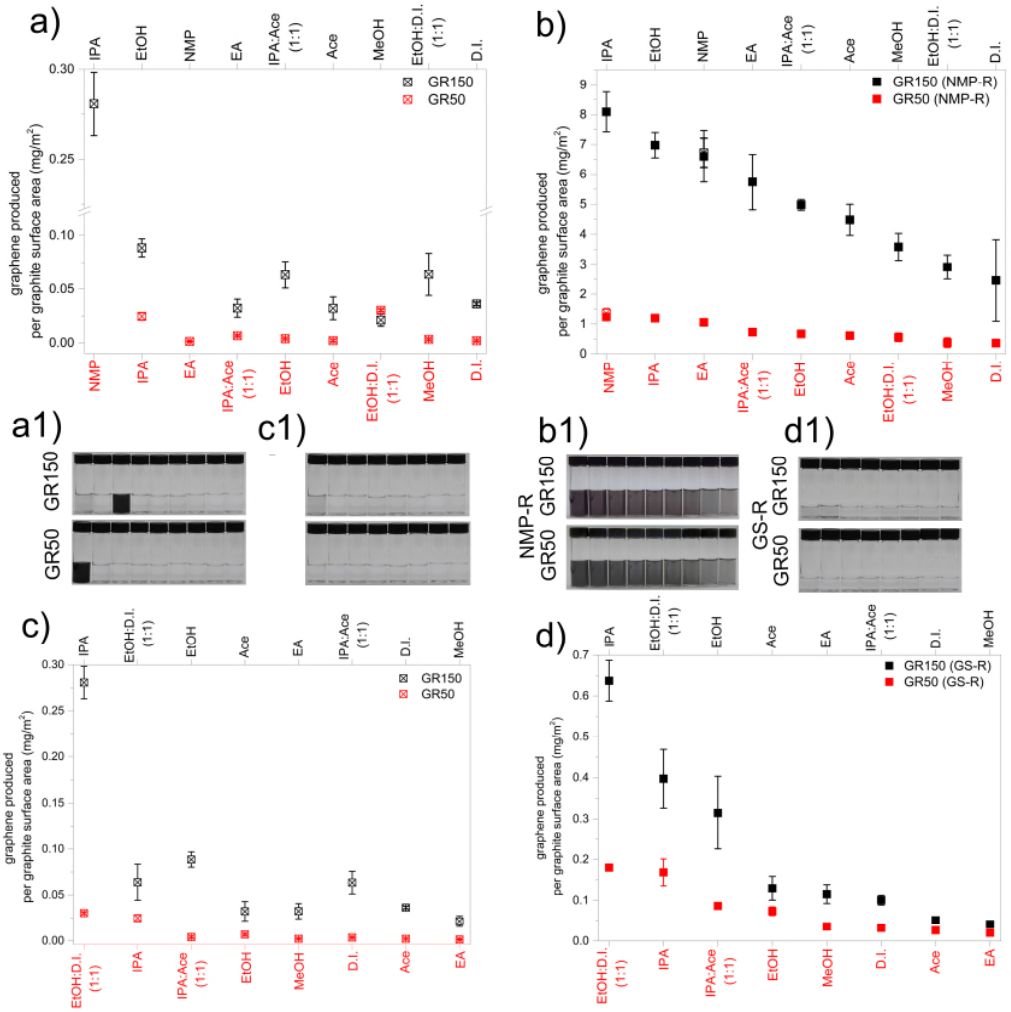

Fig. 2: *Mass of GR150 and GR50 graphene produced per surface area of G150 and G50 graphite respectively, exfoliated in various exfoliation solvent media (x-axis) determined using a) the conventional method (without redispersion) and b) NMP-R. GR 150 and GR 50 are graphene exfoliated from G150 and G50 graphite respectively. Digital images of graphene dispersion presented in a-d) are shown in a1-d1), respectively and arranged according to the solvent sequence in the x-axis of the graphs. c) Mass per surface area for NMP-exfoliated GR150 and GR50, determined through the conventional method (without redispersion) and d) the green solvent redispersion (GS-R) in selected solvents. The solvents on the x-axes of the graphs are arranged in the order of decreasing solvent exfoliation efficiency (a and b) and decreasing graphene dispersibility (c and d).*

In conventional GS-LPE, the poor graphene dispersibility of the solvents results in considerably lower graphene concentration in the supernatant after centrifugation than the actual amount of graphene produced (Fig. 2a1), This is mainly because of the inability of the green solvent to hold the graphene in the suspension. To overcome the issue of poor solvent dispersibility in assessing the actual potential or exfoliation efficiency of a green solvent for LPE, we employed a solvent exchange method, enabling the separation of exfoliation efficiency and solvent dispersibility, both contributing to the yield, *i.e.*, the actual graphene content produced (Fig. 2b1). For the NMP-R procedure, the graphene rich exfoliation product, *i.e.*, the material that is collected after exfoliation but before centrifugation, is then redispersed in NMP (Fig. 2b1) and revealing in the increase of the mass of graphene per surface area up to 29 times for IPA exfoliated GR150 and 48 times for IPA exfoliated GR50. To validate this concept, we redispersed the NMP-exfoliated GR150 and GR50 containing product back into the NMP, confirming that the concentration for both NMP-R samples remained the same (Fig. 2b, data marked with red and black arrows). This shows NMP-redispersion procedures did not impose an additional exfoliation effect, and it merely helped in dispersing the exfoliated graphene. In this work we show clear evidence for IPA possessing the highest exfoliation efficiency for both GR150 and GR50 (Fig. 2a, b). Interestingly, the exfoliation efficiencies of both, IPA and EtOH, exceeds that of NMP for GR150, whereas for GR50, the exfoliation efficiencies of IPA and EA are comparable to that of NMP (Fig. 2b, 2b1). The evaluation of the contribution of the dispersibility of the solvent towards the actual yield was employed by the GS-R method, in which the G150 and G50 were first shear-mixed in NMP (Fig. 2c and 2d), (see also S5.2). The graphene-containing suspension was then filtered and washed with EtOH in order to remove any NMP residues, dried and redispersed in selected green solvents (Fig. S1.2.2). This evaluation explicitly shows that IPA has the best graphene dispersibility for a green solvent for GR150, followed by the EtOH:D.I., whereas for GR50, EtOH:D.I. possesses better dispersibility than IPA (Fig. 2d, 2d1). It is also evident, that EA is a relatively good solvent for LPE of GR150, but not GR50 (Fig. 2d, 2d1) implying dissimilar potential of a given solvent towards different graphite types (sources) used in GS-LPE. In contrast, D.I., Ace and MeOH are generally recognised as poor solvents for exfoliation and dispersion of both, GR150 and GR50.

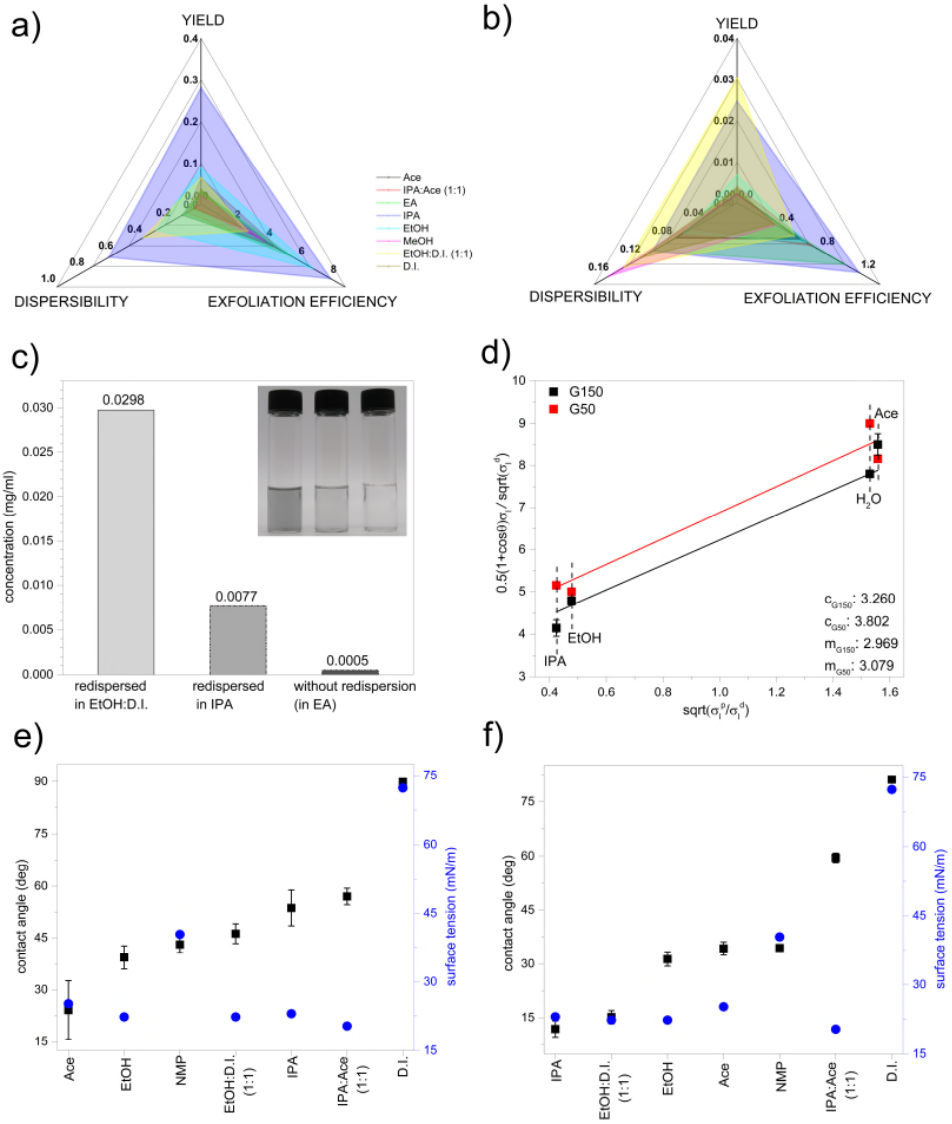

Fig. 3: *The yield of a) GR150 and b) GR50 in different solvent media, which is the combined contributions of solvent exfoliation efficiency and dispersibility. The graphene yield is determined through the conventional method. Exfoliation efficiency and graphene dispersibility are determined using the NMP-R and GS-R techniques, respectively. c) The concentration of GR50 exfoliated in EA, as compared to its redispersion in IPA and EtOH:D.I. (1:1). Inset: Digital images of dispersions correspond to the x-axis arrangement. d) The Owens-Wendt-Rabel & Kaelble model (OWRK) plot for graphite surface energy determination. The interfacial contact angle measurement e, f) evaluated by the Washburn method, between the graphite starting materials (G150 and G50) and the exfoliation solvent media listed in the x-axis. The data for G150 and G50 are shown in e) and f) respectively.*

We studied the contribution of the dispersibility and exfoliation efficiency (of green solvents) to the graphene yield for both G50 and G150 (Fig. 3a, b). IPA has the highest dispersibility and exfoliation efficiency for GR150, resulting in high graphene yield (Fig. 3a). SM-LPE in EtOH:D.I. provides higher GR50 yield than LPE in IPA, most likely because of the significant contribution of graphene dispersibility in the process (Fig. 3b). Also, the low GR50 yield in EA is mainly due to its low graphene dispersibility rather than the exfoliation efficiency (Fig. 3b). To confirm the reliability of the GS-R and NMP-R approaches, we dispersed the dried product of SM-LPE in EA, solvent of low GR50 dispersibility but high exfoliation efficiency, in the green solvents with high GR50 dispersibility *i.e.* IPA and EtOH:D.I. (the UV-Vis spectra are shown in S7). This resulted in the enhancement of GR50 yield by 16 times when redispersed in IPA (from 0.0005 mg/ml to 0.0077 mg/ml), and 60 times (from 0.0005 mg/ml to 0.0298 mg/ml) when redispersed in EtOH:D.I. (Fig. 3c) implying that the actual exfoliation efficiency of EA is higher than initially detected. All findings discussed above beg the question of what the reason behind the high exfoliation efficiency of green solvents (*e.g.* IPA) is. In order to understand the exfoliation efficiency, we studied the correlation between graphite surface energy and solvent surface tension. We employed the Washburn method and evaluated the interfacial contact angle for G50 and G150, without the need of compressing it into pellet – required for a conventional contact angle approach (Fig. S8). The contact angle obtained are used for the Owens-Wendt-Rabel & Kaelble (OWRK) plot (Fig. 3d) for graphite surface energy determination, calculated from the gradient and y-intercept of the plot. Both G50 and G150 graphite exhibit different surface energy (S8.1). The interfacial contact angle between all tested solvents and, G150 and G50, is lower than 90° (Fig. 3e), confirming the feasibility of both graphite types to be wetted, as the lower interfacial contact angle between graphite and solvent contributes to the lower interfacial surface tension. Fig. 3e,f indicates however, that not all solvents contribute to the wettability of graphite materials in the same way, even those with similar surface tension. For example NMP, known as the best solvent for exfoliating and dispersing graphene, has poorer wettability than number of the green solvents. The calculated surface energies for G150 and G50 are 19.44 and 23.93 mN/m respectively (Fig. 3d), which are close to the surface tension for most tested green solvents except D.I.. NMP however has much higher surface tension than the surface energies of both G150 and G50 and yet, it has high exfoliation efficiency. Another possible way to explain this phenomena is the concept of polar to dispersive component ratio of surface tension (σ_p/σ_d) [37,38] The polar component, $\sigma_s^{\,p}$, and dispersive component, $\sigma_s^{\,d}$, for graphite were calculated using the OWRK model (see S8). The analysis shows the difference in σ^p/σ^d between G150 and G50, and solvent ($\Delta\sigma_{(p/d)}$) (Fig. S8). $\Delta\sigma_{(p/d)}$ for NMP is lower than that for green solvents while maintaining high exfoliation efficiency, regardless of its large surface tension difference with G150 and G50 graphite. Similarly, IPA shows low $\Delta\sigma$(p/d), which explains its high exfoliation efficiency, close to that of NMP. On the contrary, acetone and D.I. show high $\Delta\sigma$(p/d), which causes the low exfoliation efficiency.

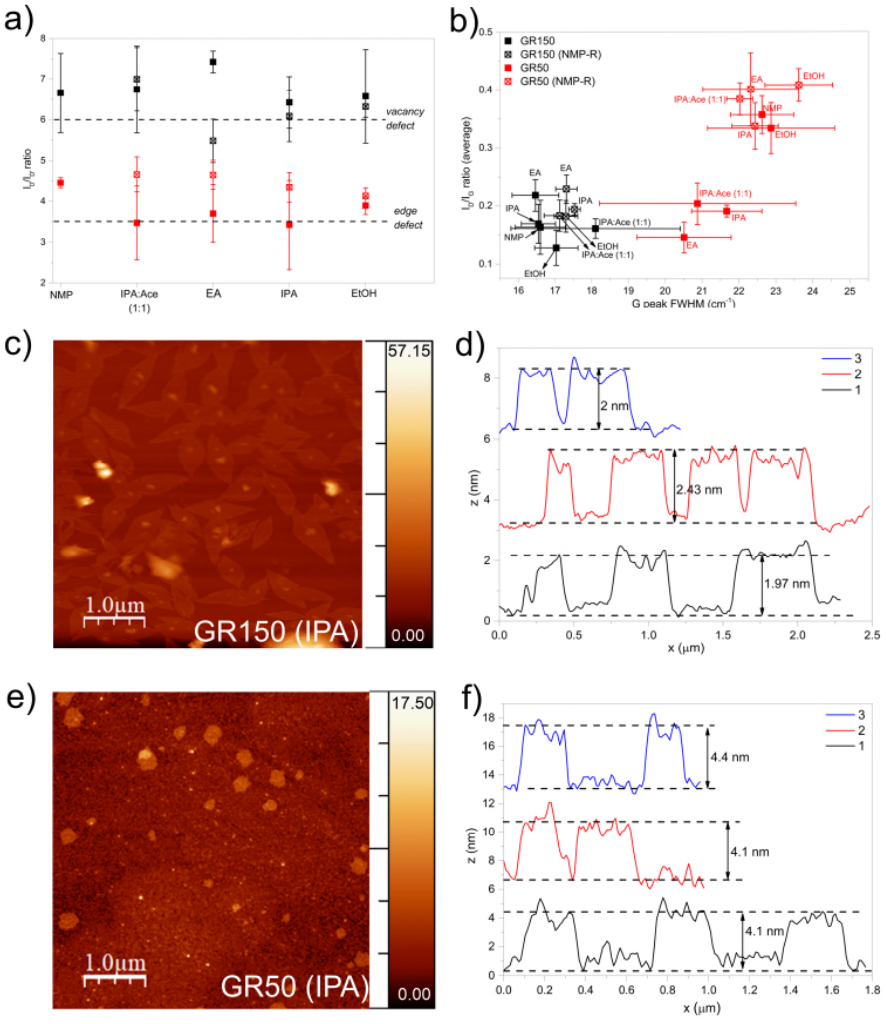

Fig. 4: *Raman spectroscopy analysis for GR150 and GR50 before and after NMP-R a) on type of defects (D/D' intensity ratio) for NMP, IPA:Ace (1:1), EA, IPA and EtOH, b) and defect density (D/G intensity ratio) against disorder (G peak FWHM). Atomic Force Microscopy thickness analysis performed on c) GR 150 and e) GR 50 exfoliated in IPA and displayed in d) and f) respectively.*

To identify the type of defects and the quality of the exfoliated graphene, the Raman spectroscopy analysis was employed. The evaluation of $I_D/I_{D'}$[39] for all exfoliated graphene samples showed that the type of defects is similar to that of NMP-R graphene, except for the EA-exfoliated GR150 (Fig. 4a). The variation of defects type and density/disorder across the samples (Fig. 4a,b) are lower for both (with shorter error bars), NMP-R GR150 and GR50, when compared to those without redispersion. We analysed the FWHM for G peak in conjunction with D to G intensity ratio (I_D/I_G) as it is confirmed to be a more accurate way to determine the lattice disorder within graphene.[40,41] The G peak FWHM is higher for GR50 exfoliated in all investigated solvents, hence GR50 has a higher lattice disorder than the GR150 (Fig. 5b). The NMP-R G50 however, is more disordered with higher defect density. This implies that NMP not only improves the dispersibility, and hence yield of graphene, but also more likely disperses the highly disordered graphene. The full Raman Spectroscopy spectra for graphene (before and after NMP-R) are shown in Fig. S9. AFM examination was used to determine the thickness of for GR150 and G50 exfoliated in IPA. The exfoliated GR150 shows very homogenous leaf-like structure with lateral size near to micron scale, and with thickness ranging from 5 to 9 layers (Fig. 4c and d). GR50 exfoliated in IPA however, has smaller lateral size but is thicker than the IPA-exfoliated GR150 (Fig. 4e and f). This is strong evidence of how the structure and morphology of initial graphite materials affect the quality and lateral size of the final product, and this must not be neglected by the graphene community.

CONCLUSIONS AND OUTLOOK

We showed direct evidence that the yield of graphene produced by LPE consists of two separate factors/components (i) the solvent exfoliation efficiency and (ii) the solvent's ability to disperse the exfoliated graphene. We systematically evaluated a wide range of green solvents and their mixtures together with the state-of-art NMP solvent, which is known as the best for LPE, as a control. Specifically, we studied the potential of NMP-R that we developed in assessing and quantifying the exfoliation efficiency of green solvents, and the GS-R in assessing the graphene dispersibility of green solvents. From the study, IPA solvent has high exfoliation efficiency towards the exfoliation of GR150 graphene, which is comparable to that of NMP (despite of it's poor graphene dispersibility), and EtOH:D.I. provides the highest GR50 yield mainly because of its good graphene dispersibility. We also verified the superior exfoliation efficiency of IPA by experimentally-studying the surface energy and surface tension between graphite and solvent using Washburn method. By redispersing the graphene exfoliated in the solvent with high exfoliation efficiency but poor dispersibility, into solvent with relatively high dispersibility, the graphene concentration can be improved up to 16 times. Our NMP-R and GS-R approaches can be applied to LPE on any type of layered material, in order to evaluate the potential of green solvents for obtaining the highest possible yield of material.

ASSOCIATED CONTENT

SUPPORTING INFORMATION

Supporting Information is available.

CORRESPONDING AUTHOR

*Nicole Grobert (nicole.grobert@materials.ac.ox.uk)

AUTHOR CONTRIBUTIONS

All authors have given approval to the final version of the manuscript. ‡These authors contributed equally.

AUTHOR ORCID NUMBERS

Kai Ling Ng (0000-0003-3476-6031); Barbara M Maciejewska (0000-0002-3101-366X), Ling Qin (0000-0003-2656-2477), Colin Johnston (0000-0001-7484-6904), Jesus Barrio (0000-0002-4147-2667), Maria-Madgalena Titirici (0000-0003-0773-2100) Iakovos Tzanakis (0000-0002-8258-1034), Dmitry G Eskin (0000-0002-0303-2249), Kyriakos Porfyrakis (0000-0003-1364-0261), Jiawei Mi (0000-0003-4923-330X), Nicole Grobert (0000-0002-8499-8749)

ACKNOWLEDGMENTS

We thank Ryan Schofield and George Tebbutt for fruitful discussions and the Oxford Materials Characterisation Services for access to equipment. This work has been funded by the UK Engineering and Physical Sciences Research Council (EPSRC), within the project "Sustainable and industrially scalable ultrasonic liquid phase exfoliation technologies for manufacturing 2D advanced functional materials" (EcoUltra2D), with the grant nos. EP/R031665/1; EP/R031401/1; EP/R031819/1; EP/R031975/1. We wish to acknowledge the support of the Henry Royce Institute for advanced materials for Kai Ling Ng, through the Student Equipment Access Scheme enabling access to Kruss GmbH K100C Surface Tensiometer facilities at the University of Manchester; EPSRC Grant Number EP/R00661X/1. Nicole Grobert thanks the Royal Society for financial support.

FUNDING SOURCES

EPSRC, The Royal Society

ABBREVIATIONS

LPE, liquid phase exfoliation; SM, shear mixing; SM-LPE, shear-mixing liquid phase exfoliation; US, ultrasonication; NMP, 1-methyl-2-pyrrolidone; DMF, dimethylformamide; GS-LPE, green solvent-liquid phase exfoliation; NMP-R, NMP-redispersion; GS-R, green solvent-redispersion; FWHM, full width half maximum; AFM, atomic force microscopy; BET, Brunauer-Emmet-Teller

REFERENCES

(1) Tran, T. S.; Dutta, N. K.; Choudhury, N. R. Graphene Inks for Printed Flexible Electronics: Graphene Dispersions, Ink Formulations, Printing Techniques and Applications. *Advances in Colloid and Interface Science*. 2018. https://doi.org/10.1016/j.cis.2018.09.003.

(2) Baker, J. A.; Worsley, C.; Lee, H. K. H.; Clark, R. N.; Tsoi, W. C.; Williams, G.; Worsley, D. A.; Gethin, D. T.; Watson, T. M. Development of Graphene Nano-Platelet Ink for High Voltage Flexible Dye Sensitized Solar Cells with Cobalt Complex Electrolytes. *Adv. Eng. Mater.* **2017**. https://doi.org/10.1002/adem.201600652.

(3) Han, S.; Sun, J.; He, S.; Tang, M.; Chai, R. The Application of Graphene-Based Biomaterials in Biomedicine. *American Journal of Translational Research*. 2019.

(4) Zang, W.; Liu, Z.; Kulkarni, G. S.; Zhu, H.; Wu, Y.; Lee, K.; Li, M. W. H.; Fan, X.; Zhong, Z. A Microcolumn DC Graphene Sensor for Rapid, Sensitive, and Universal Chemical Vapor Detection. *Nano Lett.* **2021**, *21* (24), 10301–10308. https://doi.org/10.1021/acs.nanolett.1c03416.

(5) Mori, F.; Kubouchi, M.; Arao, Y. Effect of Graphite Structures on the Productivity and Quality of Few-Layer Graphene in Liquid-Phase Exfoliation. *J. Mater. Sci.* **2018**. https://doi.org/10.1007/s10853-018-2538-3.

(6) Kozhemyakina, N. V.; Eigler, S.; Dinnebier, R. E.; Inayat, A.; Schwieger, W.; Hirsch, A. Effect of the Structure and Morphology of Natural, Synthetic and Post-Processed Graphites on Their Dispersibility and Electronic Properties. *Fullerenes Nanotub. Carbon Nanostructures* **2013**. https://doi.org/10.1080/1536383X.2012.702162.

(7) Ferguson, A.; Caffrey, I. T.; Backes, C.; Coleman, J. N.; Bergin, S. D. Differentiating Defect and Basal Plane Contributions to the Surface Energy of Graphite Using Inverse Gas Chromatography. *Chem. Mater.* **2016**. https://doi.org/10.1021/acs.chemmater.6b02721.

(8) Qin, L.; Maciejewska, B. M.; Subroto, T.; Morton, J. A.; Porfyrakis, K.; Tzanakis, I.; Eskin, D. G.; Grobert, N.; Fezzaa, K.; Mi, J. Ultrafast Synchrotron X-Ray Imaging and Multiphysics Modelling of Liquid Phase Fatigue Exfoliation of Graphite under Ultrasound. *Carbon N. Y.* **2022**, *186*, 227–237. https://doi.org/10.1016/j.carbon.2021.10.014.

(9) He, P.; Cao, J.; Ding, H.; Liu, C.; Neilson, J.; Li, Z.; Kinloch, I. A.; Derby, B. Screen-Printing of a Highly Conductive Graphene Ink for Flexible Printed Electronics. *ACS Appl. Mater. Interfaces* **2019**. https://doi.org/10.1021/acsami.9b04589.

(10) Kim, D. S.; Jeong, J. M.; Park, H. J.; Kim, Y. K.; Lee, K. G.; Choi, B. G. Highly Concentrated, Conductive, Defect-Free Graphene Ink for Screen-Printed Sensor Application. *Nano-Micro Lett.* **2021**. https://doi.org/10.1007/s40820-021-00617-3.

(11) Hernandez, Y.; Nicolosi, V.; Lotya, M.; Blighe, F. M.; Sun, Z.; De, S.; McGovern, I. T.; Holland, B.; Byrne, M.; Gun'ko, Y. K.; Boland, J. J.; Niraj, P.; Duesberg, G.; Krishnamurthy, S.; Goodhue, R.; Hutchison, J.; Scardaci, V.; Ferrari, A. C.; Coleman, J. N. High-Yield Production of Graphene by Liquid-Phase Exfoliation of Graphite. *Nat. Nanotechnol.* **2008**. https://doi.org/10.1038/nnano.2008.215.

(12) Hu, C. X.; Shin, Y.; Read, O.; Casiraghi, C. Dispersant-Assisted Liquid-Phase Exfoliation of 2D Materials beyond Graphene. *Nanoscale*. 2021. https://doi.org/10.1039/d0nr05514j.

(13) Tyurnina, A. V.; Tzanakis, I.; Morton, J.; Mi, J.; Porfyrakis, K.; Maciejewska, B. M.; Grobert, N.; Eskin, D. G. Ultrasonic Exfoliation of Graphene in Water: A Key Parameter Study. *Carbon N. Y.* **2020**. https://doi.org/10.1016/j.carbon.2020.06.029.

(14) Morton, J. A.; Khavari, M.; Qin, L.; Maciejewska, B. M.; Tyurnina, A. V.; Grobert, N.; Eskin, D. G.; Mi, J.; Porfyrakis, K.; Prentice, P.; Tzanakis, I. New Insights into Sono-Exfoliation Mechanisms of Graphite: In Situ High-Speed Imaging Studies and Acoustic Measurements. *Mater. Today* **2021**, *49* (October), 10–22. https://doi.org/10.1016/j.mattod.2021.05.005.

(15) Tyurnina, A. V.; Tzanakis, I.; Morton, J.; Mi, J.; Porfyrakis, K.; Maciejewska, B. M.; Grobert, N.; Eskin, D. G. Ultrasonic Exfoliation of Graphene in Water: A Key Parameter Study. *Carbon N. Y.* **2020**, *168* (2020), 737–747. https://doi.org/10.1016/j.carbon.2020.06.029.

(16) Tyurnina, A. V.; Morton, J. A.; Subroto, T.; Khavari, M.; Maciejewska, B.; Mi, J.; Grobert, N.; Porfyrakis, K.; Tzanakis, I.; Eskin, D. G. Environment Friendly Dual-Frequency Ultrasonic Exfoliation of Few-Layer Graphene. *Carbon N. Y.* **2021**, *185*, 536–545. https://doi.org/10.1016/j.carbon.2021.09.036.

(17) Yi, M.; Shen, Z.; Zhang, X.; Ma, S. Achieving Concentrated Graphene Dispersions in Water/Acetone Mixtures by the Strategy of Tailoring Hansen Solubility Parameters. *J. Phys. D. Appl. Phys.* **2013**. https://doi.org/10.1088/0022-3727/46/2/025301.

(18) Yi, M.; Shen, Z.; Ma, S.; Zhang, X. A Mixed-Solvent Strategy for Facile and Green Preparation of Graphene by Liquid-Phase Exfoliation of Graphite. *J. Nanoparticle Res.* **2012**. https://doi.org/10.1007/s11051-012-1003-5.

(19) O'Neill, A.; Khan, U.; Nirmalraj, P. N.; Boland, J.; Coleman, J. N. Graphene Dispersion and Exfoliation in Low Boiling Point Solvents. *J. Phys. Chem. C* **2011**. https://doi.org/10.1021/jp110942e.

(20) Vacacela Gomez, C.; Guevara, M.; Tene, T.; Villamagua, L.; Usca, G. T.; Maldonado, F.; Tapia, C.; Cataldo, A.; Bellucci, S.; Caputi, L. S. The Liquid Exfoliation of Graphene in Polar Solvents. *Appl. Surf. Sci.* **2021**. https://doi.org/10.1016/j.apsusc.2021.149046.

(21) Goulart, V. A. M.; Katia, N. Graphene-Based Nanomaterials : Biological and Medical Applications and Toxicity. **2015**.

(22) Notley, S. M. Highly Concentrated Aqueous Suspensions of Graphene through Ultrasonic Exfoliation with Continuous Surfactant Addition. *Langmuir* **2012**, *28* (40), 14110–14113. https://doi.org/10.1021/la302750e.

(23) Shin, Y.; Just-Baringo, X.; Zarattini, M.; Isherwood, L. H.; Baidak, A.; Kostarelos, K.; Larrosa, I.; Casiraghi, C. Charge-Tunable Graphene Dispersions in Water Made with Amphoteric Pyrene Derivatives. *Mol. Syst. Des. Eng.* **2019**. https://doi.org/10.1039/c9me00024k.

(24) Feng, B. B.; Wang, Z. H.; Suo, W. H.; Wang, Y.; Wen, J. C.; Li, Y. F.; Suo, H. L.; Liu, M.; Ma, L. Performance of Graphene Dispersion by Using Mixed Surfactants. *Mater. Res. Express* **2020**. https://doi.org/10.1088/2053-1591/abb2ca.

(25) Johnson, D. W.; Dobson, B. P.; Coleman, K. S. Current Opinion in Colloid & Interface Science A Manufacturing Perspective on Graphene Dispersions. *Curr. Opin. Colloid Interface Sci.* **2015**, *20* (5–6), 367–382. https://doi.org/10.1016/j.cocis.2015.11.004.

(26) Zhang, X.; Coleman, A. C.; Katsonis, N.; Browne, W. R.; Van Wees, B. J.; Feringa, B. L. Dispersion of Graphene in Ethanol Using a Simple Solvent Exchange Method. *Chem. Commun.* **2010**. https://doi.org/10.1039/c0cc02688c.

(27) Yi, M.; Shen, Z.; Liang, S.; Lei, L.; Zhang, X.; Ma, S. Water Can Stably Disperse Liquid-Exfoliated Graphene. *Chem. Commun.* **2013**. https://doi.org/10.1039/c3cc46457a.

(28) Barwich, S.; Khan, U.; Coleman, J. N. A Technique to Pretreat Graphite Which Allows the Rapid Dispersion of Defect-Free Graphene in Solvents at High Concentration. *J. Phys. Chem. C* **2013**. https://doi.org/10.1021/jp4047006.

(29) Coleman, J. N. Liquid-Phase Exfoliation of Nanotubes and Graphene. *Adv. Funct. Mater.* **2009**. https://doi.org/10.1002/adfm.200901640.

(30) Hernandez, Y.; Lotya, M.; Rickard, D.; Bergin, S. D.; Coleman, J. N. Measurement of Multicomponent Solubility Parameters for Graphene Facilitates Solvent Discovery. *Langmuir* **2010**. https://doi.org/10.1021/la903188a.

(31) Niu, L.; Coleman, J. N.; Zhang, H.; Shin, H.; Chhowalla, M.; Zheng, Z. Production of Two-Dimensional Nanomaterials via Liquid-Based Direct Exfoliation. *Small* **2016**. https://doi.org/10.1002/smll.201502207.

(32) Van Engers, C. D.; Cousens, N. E. A.; Babenko, V.; Britton, J.; Zappone, B.; Grobert, N.; Perkin, S. Direct Measurement of the Surface Energy of Graphene. *Nano Lett.* **2017**. https://doi.org/10.1021/acs.nanolett.7b01181.

(33) Hernandez, Y.; Nicolosi, V.; Lotya, M.; Blighe, F. M.; Sun, Z.; De, S.; McGovern, I. T.; Holland, B.; Byrne, M.; Gun'ko, Y. K.; Boland, J. J.; Niraj, P.; Duesberg, G.; Krishnamurthy, S.; Goodhue, R.; Hutchison, J.; Scardaci, V.; Ferrari, A. C.; Coleman, J. N. High-Yield Production of Graphene by Liquid-Phase Exfoliation of Graphite. *Nat. Nanotechnol.* **2008**, *3* (9), 563–568. https://doi.org/10.1038/nnano.2008.215.

(34) Coleman, J. N.; Lotya, M.; O'Neill, A.; Bergin, S. D.; King, P. J.; Khan, U.; Young, K.; Gaucher, A.; De, S.; Smith, R. J.; Shvets, I. V.; Arora, S. K.; Stanton, G.; Kim, H. Y.; Lee, K.; Kim, G. T.; Duesberg, G. S.; Hallam, T.; Boland, J. J.; Wang, J. J.; Donegan, J. F.; Grunlan, J. C.; Moriarty, G.; Shmeliov, A.; Nicholls, R. J.; Perkins, J. M.; Grieveson, E. M.; Theuwissen, K.; McComb, D. W.; Nellist, P. D.; Nicolosi, V. Two-Dimensional Nanosheets Produced by Liquid Exfoliation of Layered Materials. *Science (80-.).* **2011**, *331* (6017), 568–571. https://doi.org/10.1126/science.1194975.

(35) Xu, Y.; Cao, H.; Xue, Y.; Li, B.; Cai, W. Liquid-Phase Exfoliation of Graphene: An Overview on Exfoliation Media, Techniques, and Challenges. *Nanomaterials*. 2018. https://doi.org/10.3390/nano8110942.

(36) Lund, S.; Kauppila, J.; Sirkiä, S.; Palosaari, J.; Eklund, O.; Latonen, R. M.; Smått, J. H.; Peltonen, J.; Lindfors, T. Fast High-Shear Exfoliation of Natural Flake Graphite with Temperature Control and High Yield. *Carbon N. Y.* **2021**. https://doi.org/10.1016/j.carbon.2020.11.094.

(37) Shen, J.; He, Y.; Wu, J.; Gao, C.; Keyshar, K.; Zhang, X.; Yang, Y.; Ye, M.; Vajtai, R.; Lou, J.; Ajayan, P. M. Liquid Phase Exfoliation of Two-Dimensional Materials by Directly Probing and Matching Surface Tension Components. *Nano Lett.* **2015**. https://doi.org/10.1021/acs.nanolett.5b01842.

(38) Wang, M.; Xu, X.; Ge, Y.; Dong, P.; Baines, R.; Ajayan, P. M.; Ye, M.; Shen, J. Surface Tension Components Ratio: An Efficient Parameter for Direct Liquid Phase Exfoliation. *ACS Appl. Mater. Interfaces* **2017**. https://doi.org/10.1021/acsami.6b16578.

(39) Eckmann, A.; Felten, A.; Mishchenko, A.; Britnell, L.; Krupke, R.; Novoselov, K. S.; Casiraghi, C. Probing the Nature of Defects in Graphene by Raman Spectroscopy. *Nano Lett.* **2012**. https://doi.org/10.1021/nl300901a.

(40) Ferrari, A. C. Raman Spectroscopy of Graphene and Graphite: Disorder, Electron-Phonon Coupling, Doping and Nonadiabatic Effects. *Solid State Commun.* **2007**, *143* (1–2), 47–57. https://doi.org/10.1016/j.ssc.2007.03.052.

(41) Bracamonte, M. V.; Lacconi, G. I.; Urreta, S. E.; Foa Torres, L. E. F. On the Nature of Defects in Liquid-Phase Exfoliated Graphene. *J. Phys. Chem. C* **2014**. https://doi.org/10.1021/jp501930a.